NOVEL NANOPARTICLES SHELLED WITH CHITOSAN FOR ORAL DELIVERY OF PROTEIN DRUGS

Yu-Hsin Lin[1] / Chiung-Tong Chen[2] / Hsiang-Fa Liang[1] / Po-Hong Lee[1] / Fwu-Long Mi[3] / Hsing-Wen Sung[1]*

[1]Department of Chemical Engineering, National Tsing Hua University, Hsinchu, Taiwan 30013, ROC

[2]Division of Biotechnology and Pharmaceutical Research, National Health Research Institutes, Taipei, Taiwan, ROC

[3]Division of Applied Chemistry, Department of Applied Science, Chinese Naval Academy, Kaohsiung, Taiwan, ROC

Abstract

Production of pharmaceutically active proteins, like insulin, in large quantities has become feasible. The oral route is considered to be the most convenient way of drug administrations for patients. Nevertheless, the intestinal epithelium is a major barrier to the absorption of hydrophilic drugs such as proteins because they cannot diffuse across the cells through the lipid-bilayer cell membranes. Therefore, attentions have been given to improving paracellular transport of hydrophilic drugs. The transport of hydrophilic molecules via the paracellular pathway is, however, severely restricted by the presence of tight junctions which are located at the luminal aspect of adjacent epithelial cells. It is known that chitosan has special features of adhering to the mucosal surface and transiently opening the tight junctions between cells. In the study, a novel nanoparticle system was prepared using a simple and mild ionic-gelation method upon addition of a hydrolyzed poly-γ-glutamic acid solution into a low molecular-weight chitosan solution. The particle size and zeta potential value of the prepared nanoparticles can be controlled by their constituted compositions. The results of the prepared nanoparticles obtained by TEM showed that the morphology of the prepared nanoparticles was spherical in shape. Evaluation of the prepared nanoparticles in enhancing the intestinal paracellular transport was investigated *in vitro* on Caco-2 cell monolayers confirmed that the nanoparticles with chitosan dominated on the surface were able to open the tight junctions between Caco-2 cells and allowed transport of the nanoparticles via the paracellular pathways. Oral intake of insulin in the form of nanoparticles demonstrated a sustained effect of decreasing the blood glucose level over a longer period of time, at least 10 h. These results clearly showed the ability of the prepared nanoparticles to enhance the intestinal absorption of fully functional insulin.

Keywords: hydrophilic drugs; nanoparticle; ionic-gelation; paracellular transport; tight junction; diabetic rats

Introduction

Production of pharmaceutically active peptides and proteins in large quantities has become feasible [1]. The oral route is considered to be the most convenient way of drug administrations for patients. Nevertheless, the intestinal epithelium is a major barrier to the absorption of hydrophilic drugs such as peptides and proteins [2]. This is because hydrophilic drugs cannot diffuse across the cells through the lipid-bilayer cell membranes. Therefore, attentions have been given to improving

paracellular transport of hydrophilic drugs [3]. The transport of hydrophilic molecules via the paracellular pathway is, however, severely restricted by the presence of tight junctions which are located at the luminal aspect of adjacent epithelial cells [4]. These tight junctions form a barrier that limits the paracellular diffusion of hydrophilic molecules. Polymeric nanoparticles have been widely investigated as a carrier for drug delivery [5]. Among them, much attention has been paid to the nanoparticles made of synthetic biodegradable polymers such as poly-ε-caprolactone and polylactide due to their good biocompatibility [6]. However, these nanoparticles are not ideal carriers for hydrophilic drugs because of their hydrophobic property. In this study, a novel nanoparticle system, composed of hydrophilic chitosan (CS) and poly-γ-glutamic acid (γ-PGA) hydrogels, was prepared by a simple ionic-gelation method. This technique is promising as the nanoparticles can be prepared under mild conditions without using harmful solvents. It is known that organic solvents may cause degradation of peptide or protein drugs that are unstable and sensitive to their environments [7]. Additionally, Physicochemical characteristics of the prepared nanoparticles were examined by Fourier transformed infrared (FT-IR) spectroscopy, dynamic light scattering (DLS), transmission electron microscopy (TEM), and atomic force microscopy (AFM). Evaluation of the prepared nanoparticles in enhancing intestinal paracellular transport was investigated *in vitro* in Caco-2 cell monolayers. Monolayers of Caco-2 cells, derived from human colorectal adenocarcinoma, have been widely accepted as a potent *in vitro* model to predict intestinal drug permeability in humans.[19] The alternation of transepithelial electrical resistance (TEER) for the tightness of the cell layer was measured and the paracellular transport of nanoparticles was visualized using confocal laser scanning microscopy (CLSM).

Material and Methods

Chitosan with a MW of about 50 kDa was obtained by depolymerizing a commercially available chitosan using cellulase at pH 5.0 for 12 h at 37℃. After washing and ultracentrifugation, the obtained low-viscosity chitosan was collected and used for preparation of nanoparticles. γ-PGA was produced by microbial fermentation (*B. licheniformis*, ATCC 9945) at pH 6.5 for 40 h at 37℃. The MW of the purified γ-PGA obtained via the previous procedure was about 160 kDa. The aqueous γ-PGA solution was desalted by dialysis (MWCO: 100000, Spectrum Laboratories, Inc., Laguna Hills, CA) against distilled water for 12 h with water exchanges several times, and finally was lyophilized to obtain pure γ-PGA. The purified γ-PGA was confirmed by the proton nuclear magnetic resonance (^{1}H-NMR) and the FT-IR analyses.

Nanoparticles were obtained upon addition of a γ-PGA aqueous solution (pH 7.4, 2 ml), using a pipette (0.5-5 ml, PLASTIBRAND®, BrandTech Scientific lnc., Germany), into a low-MW CS aqueous solution (pH 6.0, 10 ml) at varying concentrations (0.01%, 0.05%, 0.10%, 0.15%, or 0.20% by w/v) under magnetic stirring at room temperature. Nanoparticles were collected by ultracentrifugation at 38000 rpm for 1 h. Supernatants were discarded and nanoparticles were resuspended in deionized water for further studies. FT-IR was used to analyze peak variations of amino groups of low-MW CS and carboxylic acid salts of γ-PGA in the CS–γ-PGA nanoparticles. The size distribution and zeta potential of the prepared nanoparticles were measured by dynamic light scattering (Zetasizer 3000HS). The morphological examination of the CS–γ-PGA nanoparticles was performed by TEM and AFM. To show that the paracellular transport was enhanced effectively under the influence of the prepared nanoparticles, CS-γ-PGA nanoparticles were studied in the *in vitro* model (Caco-2 cell monolayers). The paracellular transport of nanoparticles were visualized using CLSM. This method allows for optical sectioning of the transport pathways through the cell monolayer.

Results and Discution

In the study, cellulase was employed to depolymerize a commercially available CS (MW ~280 kDa, Figure 1a). It is known that cellulase catalyzes the cleavage of the glycosidic linkage in CS. The low-MW CS used in the study was obtained by precipitating the depolymerized CS solution with

aqueous NaOH at pH 7.0-7.2. Thus obtained low-MW CS had a MW of about 50 kDa (Figure 1a). The purified γ-PGA obtained from fermentation was analyzed by GPC, ^{1}H-NMR, and FT-IR. As analyzed by GPC (Figure 1b), the purified γ-PGA had a MW of ~160 kDa. In the FT-IR spectrum (Figure 2a), a characteristic peak at 1615 cm^{-1} for the associated carboxylic acid salt ($–COO^-$ antisymmetric stretch) on γ-PGA was observed. The characteristic absorption due to C=O in secondary amides (amide I band) was overlapped by the characteristic peak of $–COO^-$. Additionally, the characteristic peak observed at 3400 cm^{-1} was the N-H stretch of γ-PGA. In the ^{1}H-NMR spectrum (Figure 2b), six chief signals were observed at 1.73 and 1.94 ppm (β-CH_2), 2.19 ppm (γ-CH_2), 4.14 ppm (α-CH), 8.15 ppm (amide), and 12.58 ppm (COOH). These results indicated that the observed FT-IR and ^{1}H-NMR spectra correspond well to those expected for γ-PGA.

The Figure 3 shows the FT-IR spectra of the low-MW CS and the CS–γ-PGA nanoparticles. As shown in the spectrum of CS, the characteristic peak observed at 1563 cm^{-1} was the protonated amino group ($–NH_3^+$ deformation) on CS. In the spectrum of CS–γ-PGA complex, the characteristic peak at 1615 cm^{-1} for $–COO^-$ on γ-PGA disappeared and a new peak at 1586 cm^{-1} appeared, while the characteristic peak of $–NH_3^+$ deformation on CS at 1563 cm^{-1} shifted to 1555 cm^{-1}. These observations can be attributed to the electrostatic interaction between the negatively charged carboxylic acid salts ($–COO^-$) on γ-PGA and the positively charged amino groups ($–NH_3^+$) on CS. The electrostatic interaction between the two polyelectrolytes (γ-PGA and CS) instantaneously induced the formation of long hydrophobic segments (or at least segments with a high density of neutral ion-pairs), and thus resulted in highly neutralized complexes that segregated into colloidal nanoparticles.

The particle sizes and the zeta potential values of CS–γ-PGA nanoparticles, prepared at varying concentrations of γ-PGA and CS, were determined and the results are shown in Table 1a and 1b. When the amount of CS molecules exceeded that of local γ-PGA molecules, some of the excessive CS molecules were entangled onto the surfaces of CS-γPGA nanoparticles. Thus, the resulting nanoparticles may display a structure of a neutral polyelectrolyte-complex core surrounded by a positively charged CS shell (Table 1b) ensuring the colloidal stabilization. In contrast, as the amount of local γ-PGA molecules sufficiently exceeded that of surrounding CS molecules, the formed nanoparticles had γ-PGA exposed on the surfaces and thus had a negative charge of zeta potential. Therefore, the particle size and the zeta potential value of the prepared CS–γ-PGA nanoparticles can be controlled by their constituted compositions. The results obtained by the TEM and AFM examinations showed that the morphology of the prepared nanoparticles was spherical in shape with a smooth surface (Figure 4a and 4b).

Effects of the prepared CS–γ-PGA nanoparticles on the TEER values of Caco-2 cell monolayers are shown in Figure 5. As shown, the prepared nanoparticles with a positive surface charge were able to reduce the values of TEER of Caco-2 cell monolayers significantly. This indicated that the nanoparticles with CS dominated on the surfaces could effectively open the tight junctions between Caco-2 cells, resulting in a decrease in the TEER values. After removal of the incubated nanoparticles, a gradual increase in TEER values was noticed. In contrast, the TEER values of Caco-2 cell monolayers incubated with the nanoparticles with a negative surface charge showed no significant differences as compared to the control group. This indicated that γ-PGA does not have any effects on the opening of the intercellular tight junctions.

CLSM was used to visualize the transport of the fluorescence-labeled CS–γ-PGA (fCS–γ-PGA) nanoparticles across the Caco-2 cell monolayers and mice intestine. It shows the fluorescence images of 4 optical sections of a Caco-2 cell monolayer that had been incubated with the fCS–γ-PGA nanoparticles with a positive surface charge (zeta potential: ~30 mV) for 20 and 60 min, respectively. As shown, after 20 min of incubation with the nanoparticles, intense fluorescence signals at intercellular spaces were observed at depths of 0 and 5 μm from the apical (upper) surface of the cell monolayer. The intensity of fluorescence became weaker at levels deeper than 10 μm from the apical surface of the cell monolayer and was almost absent at depths ≧ 15 μm (Figure 6a).

After 60 min of incubation with the nanoparticles, the intensity of fluorescence observed at intercellular spaces was stronger and appeared at a deeper level than those observed at 20 min after incubation (Figure 6b).

References

[1] Liang HF, Hong MH, Ho RM, Chung CK, Lin YH, Chen CH, Sung HW. 2004. Biomacromolecules., 5: 1917-1925.

[2] Borchard G, Lueßen HL, de Boer AG, Verhoef JC, Lehr CM, Junginger HE. 1996. J. Control. Release., 39: 131-138.

[3] Kotzé AF, Lueßen HL, de Leeuw BJ, de Boer (A)BG, Verhoef JC, Junginger HE. 1998. J. Control. Release., 51: 35-46.

[4] Ballard ST, Hunter JH, Taylor AE. 1995. Annu. Rev. Nutr., 15: 35-55.

[5] Hu Y, Jiang X, Ding Y, Ge H, Yuan Y, Yang C. 2002. Biomaterials., 23: 3193-3201.

[6] Guzman M, Aberturas MR, Rodriguez-Puyol M, Molpeceres J. 2000. Drug Delivery., 7: 215-222.

[7] Kajihara M, Sugie T, Hojo T, Maeda H, Sano A, Fujioka K, Sugawara S, Urabe Y. 2001. J. Control. Release., 73: 279-291.

Table 1a : Effects of concentrations of γ-PGA and CS on the particle sizes of the prepared CS-γ-PGA nanoparticles (CS: chitosan; γ-PGA: poly-γ-glutamic acid).

Mean Particle Size (nm, n = 5)					
γ-PGA \ **CS**	0.01% [a]	0.05%	0.10%	0.15%	0.20%
0.01% [b]	79.0 ± 3.0	103.1 ± 4.6	96.7 ± 1.9	103.6 ± 1.9	140.5 ± 2.0
0.05%	157.4 ± 1.7	120.8 ± 3.9	144.5 ± 2.4	106.2 ± 3.8	165.4 ± 1.7
0.10%	202.2 ± 3.1	232.6 ± 1.2	161.0 ± 1.8	143.7 ± 2.7	218.1 ± 4.1
0.15%	277.7 ± 3.2	264.9 ± 2.1	188.6 ± 2.9	178.0 ± 2.2	301.1 ± 6.4
0.20%	284.1 ± 2.1	402.2 ± 4.0	▲	225.5 ± 3.1	365.5 ± 5.1

Table 1b : Effects of concentrations of γ-PGA and CS on the zeta potential values of the prepared CS–γ-PGA nanoparticles (CS: chitosan; γ-PGA: poly-γ-glutamic acid).

Zeta Potential (mV, n = 5)					
γ-PGA \ CS	0.01% [a]	0.05%	0.10%	0.15%	0.20%
0.01% [b]	15.4 ± 0.3	22.8 ± 0.5	19.8 ± 1.5	16.5 ± 1.4	17.2 ± 1.6
0.05%	-32.7 ± 0.7	23.7 ± 1.7	27.6 ± 0.7	20.3 ± 0.8	19.2 ± 0.6
0.10%	-33.1 ± 1.3	21.1 ± 1.6	20.3 ± 1.1	23.6 ± 0.9	24.7 ± 1.2
0.15%	-33.2 ± 2.1	-21.9 ± 2.0	19.2 ± 0.4	16.9 ± 1.7	19.8 ± 0.3
0.20%	-34.5 ± 0.5	-34.6 ± 0.3	▲	14.6 ± 0.7	16.3 ± 0.7

[a] concentration of CS (by w/v) [b] concentration of γ-PGA (by w/v) ▲ precipitation of aggregates was observed

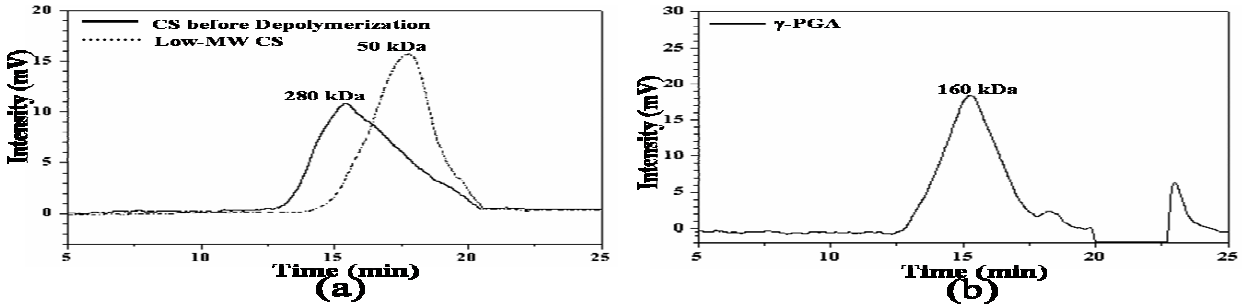

Figure 1 : GPC chromatograms of (a) CS before depolymerization and the low-MW CS used in the study; (b) γ-PGA obtained from microbial fermentation

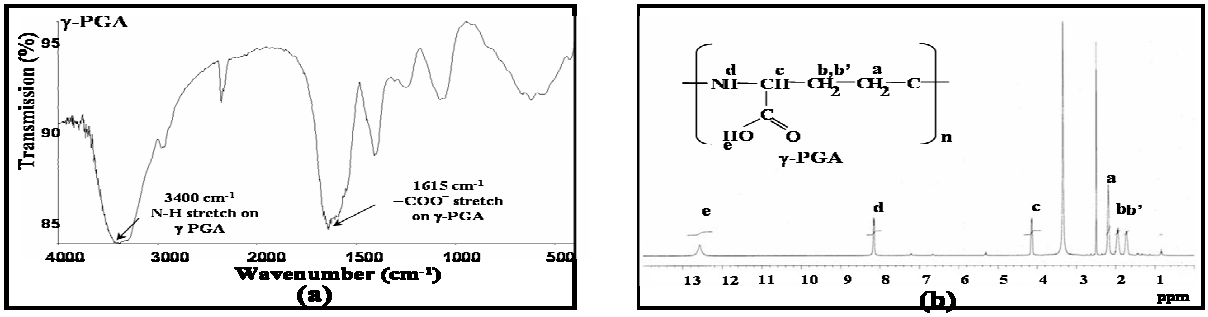

Figure 2 : FTIR and (b) ^{1}H-NMR spectra of the purified γ-PGA obtained from microbial fermentation.

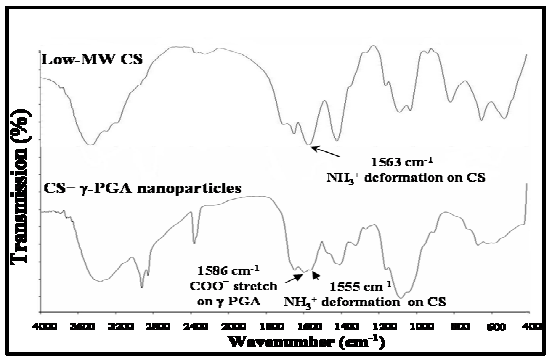

Figure 3: FT-IR of the low-MW CS and the nanoparticles.

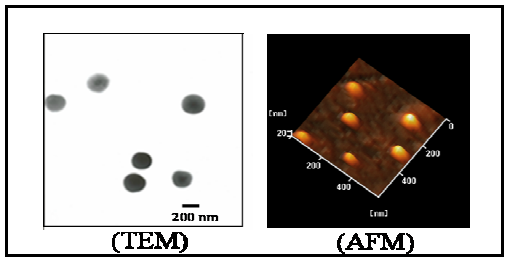

Figure 4 : The micrograph of the nanoparticles.

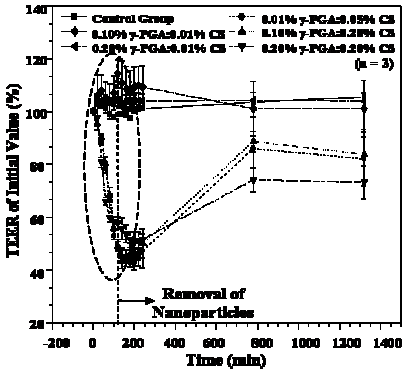

Figure 5 : Effects of the prepared nanoparticles on the TEER values of Caco-2 cell monolayers.

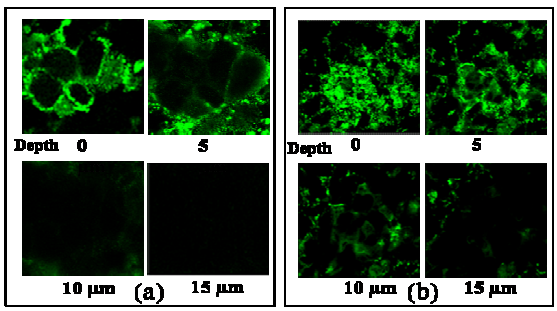

Figure 6 : Fluorescence images of the nanoparticles with with a positive surface charge for (a) 20 min and (b) 60 min.